DEVELOPMENT OF RELIABLE NARX MODELS OF GAS TURBINE COLD, WARM AND HOT START-UP

Hilal Bahlawan[1], Mirko Morini[2], Michele Pinelli[1], Pier Ruggero Spina[1], Mauro Venturini[1]

[1]Dipartimento di Ingegneria, Università degli Studi di Ferrara, Ferrara, Italy
[2]Dipartimento di Ingegneria e Architettura, Università degli Studi di Parma, Parma, Italy

ABSTRACT

This paper documents the set-up and validation of nonlinear autoregressive exogenous (NARX) models of a heavy-duty single-shaft gas turbine.

The data used for model training are time series datasets of several different maneuvers taken experimentally on a gas turbine General Electric PG 9351FA during the start-up procedure and refer to cold, warm and hot start-up. The trained NARX models are used to predict other experimental datasets and comparisons are made among the outputs of the models and the corresponding measured data.

Therefore, this paper addresses the challenge of setting up robust and reliable NARX models, by means of a sound selection of training datasets and a sensitivity analysis on the number of neurons. Moreover, a new performance function for the training process is defined to weigh more the most rapid transients. The final aim of this paper is the set-up of a powerful, easy-to-build and very accurate simulation tool which can be used for both control logic tuning and gas turbine diagnostics, characterized by good generalization capability.

NOMENCLATURE

c	weights of the error weight function
EWF	error weight function
e	error
F	performance function
f	NARX model transfer function
g	function
GN	guess number
M	mass flow rate
mse	mean square error
NI	normalization interval
N	rotational speed
n	number
nx	number of input delays
ny	number of output delays
p	stagnation pressure
P_{rC}	compressor pressure ratio
RMSE	root mean square relative error
T	temperature
TE	testing dataset
TR	training dataset
TIT	turbine inlet temperature
TOT	turbine outlet temperature
t	time
W	neural network weight
x	externally determined input variable
y	output variable
ϕ	input or output parameter

Subscripts

01	compressor inlet section
02	compressor outlet section
04	turbine outlet section

C	cold
f	fuel
H	hot
m	measured
min	minimum
max	maximum
R	relative
s	simulated
TR	number of training datasets
W	warm

INTRODUCTION

To address the challenge of modeling gas turbine (*GT*) start-up, white-box, grey-box and black-box models can be considered as the main categories of system models. White-box models are usually used with coupled and dynamics equations, thermodynamic relations, energy balance and linearization methods [1]. Instead, black-box models, such as *nonlinear autoregressive models with exogenous inputs* (*NARX*), are used when there is not enough information about the physics of the system or when is not possible to access complex dynamic equations or properly tune model parameters [1]. Moreover, grey and black box models are usually characterized by shorter calculation time and simpler parameterization.

To setup a black-box model, different types of neural networks can be trained on the basis of the different system parameters within its operating range. Before selecting the most suitable modeling approach, it is necessary to perform an analysis of the entire system (in this paper, a gas turbine) which includes the measurable parameters, monitoring system, condition and reliability of the sensors, system history recording, data system accessibility, performance curves availability, technical characteristics. The selected modeling approach should be consistent with research expectations.

Recently, *Artificial Neural Networks* (*ANN*) have been widely employed for modeling and simulation of industrial systems. As a model based on data, ANN is one of the most significant black-box modeling methods. It includes different approaches, among which the NARX. As a recurrent neural network, a NARX model has the ability to capture the dynamics of complex systems such as GTs. Such a simulator can be used for the design and production optimization of gas turbines, as well as the operation and maintenance of GTs.

In the area of black-box models specifically constructed for heavy-duty gas turbines, one can refer to the research activities carried out by Lazzaretto and Toffolo [5], Ogaji et al. [6], Arriagada et al. [7], Basso et al. [8], Bettocchi et al. [9-10], Spina and Venturini [11], Simani and Patton [12], Yoru et al. [13], Fast et al. [14-15], Fast and Palme [16] and Fast [17]. As can be seen from the literature review, most of the black-box models were built to model the steady-state operation of a gas turbine systems, i.e. after they have passed the start-up phase and have reached the stationary phase. Whereas, there is a limited number of studies related to modeling GTs during start-up. Asgari et al. [18] presented NARX models for simulation of a heavy duty single shaft gas turbine during the start-up procedure. The NARX models were capable of capturing system dynamics during start-up operation of the gas turbine and predicting the GT behavior. Some of the authors improved the NARX models developed in [18]. In fact, on average, the NARX models developed in [20] could reproduce the GT dynamic behavior more accurately (i.e. with a lower RMSE) than the NARX models presented in [18] with reference to cold start-up simulation, thanks to the optimization of the training.

The importance of GTs start-up procedure and its effect on the performance and lifetime is a strong motivation to work in this field. There are still many unforeseen events during start-up process which can arise from complex dynamics of gas turbines. Therefore, many research activities should be still carried out to fill the existing information gaps in the literature and to develop such black-box models.

Based on the literature review and by making use of experimental data for training and validation, a novel approach is proposed in this paper for simulating the dynamics of a single shaft gas turbine by means of NARX models. An extensive comparative study between real and simulated behavior is conducted to verify and validate that the proposed models can accurately predict GT dynamics during the start-up procedure. Modeling and simulation are performed on the basis of experimental time series datasets obtained from a heavy duty GT. The use of this modeling approach, which uses as input only the variables at antecedent time step (i.e. no information on the current time step is required), allows the setting up of a powerful simulation tool that can also be used for the real time control and diagnostics of GT sensors.

The main contribution of this paper is a general methodology for training NARX models. The methodology consists of three main steps:

- Selection of the training datasets which must include both fast and slow input variations;
- Definition of an error weight function which is aimed at forcing the NN to reproduce the most relevant transients;
- Sensitivity analysis on the number of neurons and initial weights to identify the NN with lowest RMSE.

The trained NARX models prove reliable to reproduce GT dynamics, in particular the start-up phase. Moreover, they are suitable to be implemented in real time applications since they do not require high computational effort. However, as a common feature of all black box models, the use of NARX models is recommended within the range of values in which were trained.

LITERATURE REVIEW

Different types of gas turbines have been modeled so far by using ANN. The model under consideration may be a micro gas turbine, an aero gas turbine or an industrial power plant gas turbine including heavy-duty industrial gas turbines, which is the subject of this study. In paper [2] ANNs were used to model the steady state operation of small scale combined heat and power micro gas turbine for monitoring purposes. A micro gas turbine plant was also modeled by Sisworahardjo and El-Sharkh [3] by using multilayer feedforward ANN with back-propagation training. Feed-forward neural network based on Gaussian kernel function was capable to predict the compressor performance map, both in case of interpolation and extrapolation [4]. Also in [19], the authors explored the transient behavior of a heavy-duty gas turbine by developing and comparing two different approaches, a physics-based and black box approach by using Simulink and NARX models respectively. The results showed that both Simulink and NARX models are capable of satisfactory prediction.

Dominiczak et al. [21] considered NARX model of a steam turbine to perform an on-line prediction of temperature and stress in steam turbine components. Vatani et al. [22] developed two methodologies, i.e. NARX neural network and recurrent neural network (RNN), for degradation prognosis and health monitoring of gas turbine engines using dynamic neural networks. They showed that the prediction errors of NARX neural networks are lower compared to the RNN architecture.

Fault detection and isolation task of a gas turbine engine was addressed in [23], identifying gas turbine engine dynamics by using a fleet of neural networks. Fault detection of temperature sensors in a heavy duty gas turbine was also the purpose of the paper [24] where the authors attempted to predict the outlet temperature of a GT by using Laguerre network-based hierarchical fuzzy system models. The state of a gas turbine engine in aircraft was estimated by Lakshmi et al. [25], by using neural network algorithms. Sina et al. [26] designed and developed a fault detection and isolation scheme for aircraft gas turbine by using dynamic neural networks. They found that their proposed scheme represents a promising tool for aircraft engine diagnostics and health monitoring. Tsoutsanis et al. [27] proposed and developed a novel scheme for prognostics of industrial gas turbines operating under dynamic conditions. They presented the results of their methodology for detecting and predicting the performance of gas turbine components. Nonparametric and parametric models of a turbojet engine prototype were presented by Tavakolpour-Saleh et al. in [28]. The system identification procedure was conducted to find the best model that fits the nonlinear relationship between the fuel flow rate as the input and the rotational speed of the engine as the output. They demonstrated that the nonparametric model using NARX models was preferable with respect to the parametric one.

Many other white-box and black-box methods for simulating the transient behavior of gas turbine individual components (such as compressors) were presented in literature. The authors also contributed to this field of research. For instance, one can refer to the neural network techniques used by Venturini [29, 30] to explore the transient behavior of compressors. Similar studies were carried out by Venturini [31] and Morini et al. [32, 33] by using white-box methods. Nowak et al. [34] also used two ANNs working in series to control the steam turbine start-up process. They achieved prediction errors of about 20%.

GAS TURBINE START-UP

The start-up period is the gas turbine operating time until steady state combustion conditions are reached. GTs are not self-starting and require to be cranked from an external source as an electric or Diesel motor to start working. The starter is used until the GT speed reaches a prescribed percentage of the rated speed. GT start up procedure can be divided into four stages, including dry cranking, purging, light-off and acceleration to idle [35, 36]. During dry cranking, the motor shaft is rotated by the starter system without any fuel supply. After cranking, purging (removal of combustible gas/fuel in the gas path) takes place. In this phase, the rotational speed is kept at a constant value with a proper mass flow rate through the combustion chamber, the turbine and the heat recovery steam generator. Then, in the light-off phase, the fuel is supplied to the combustor and igniters are excited. This causes a local start ignition within the combustor, followed by light-around of all the burners. At the end, in the acceleration to idle phase, the fuel mass flow rate is further increased and the rotational speed increases towards the idle value.

TRAINING METHODOLOGY

A NARX model is an autoregressive, recurrent and dynamic neural network with exogenous inputs. It includes feedback connections which build-up different network layers and therefore it is mainly used in time series modelling. The following equation relates NARX model output to its inputs:

$$y(t) = f[x(t-1),..., x(t-nx), y(t-1),..., y(t-ny)] \qquad (1)$$

where y is the output variable and x is an exogenous input. From Eq. (1), it can be seen that the value of the dependent output signal y at time t is regressed on previous output values (back to the time point t-ny) and previous values of an independent exogenous input signals x (back to the time point t-nx).

It is important to highlight that both output and exogenous inputs are evaluated at antecedent time step, i.e. no information on the current time step is required.

For this reason, NARX models are mainly used for modelling nonlinear dynamic systems [37]. In addition, they can be used as a predictor, to predict the next value of the input signal, and also for non-linear filtering of noisy input signals.

The flowchart of the methodology set-up in this paper for NARX model development is shown in Figure 1. The training methodology is made up of three steps, i.e. selection of the training datasets, definition of an error weight function and a sensitivity analysis on the number of neurons and initial neurons weights.

Selection of the training datasets

The first step of the methodology consists of the selection of the training datasets. The training datasets should be selected in such a manner that the resulting NARX model can generalize well in the operating range of the GT during the start-up procedure. Namely, to set up a robust NARX model, the rate of change of the training maneuvers used for training must include the most rapid variation and the slowest variation.

Therefore, the training datasets should cover the whole operating range of the GT and include the maximum and minimum values of all the inputs and outputs.

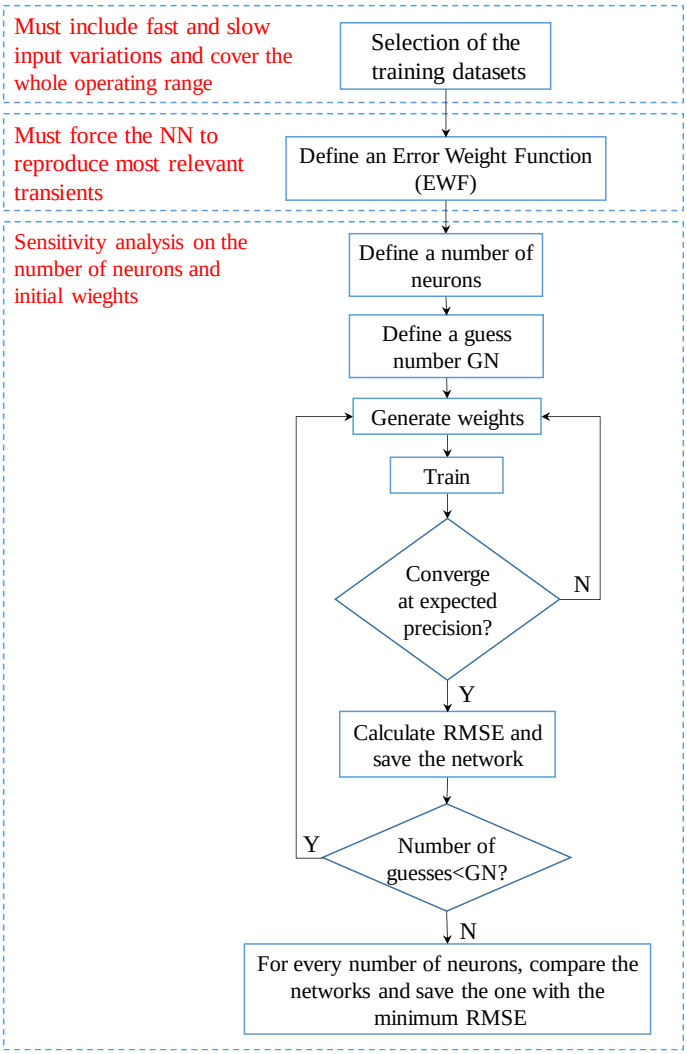

Figure 1 – Methodology for NARX model training

Definition of an Error Weight Function (EWF)

The second step of the training methodology (see Figure 1) is the definition of an error weight function which allows the NN to reproduce the most relevant transients.

According to [37], Eq. (2) reports the function (mean square error - *mse*) which is commonly adopted for defining neural network performance during training:

$$F = mse = \frac{1}{n}\sum_{i=1}^{n}\left(e_i\right)^2 = \frac{1}{n}\sum_{i=1}^{n}\left(y_{mi} - y_{si}\right)^2 \qquad (2)$$

where *n* is the number of data in each dataset.

In the default performance function, i.e. Eq. (2), all squared errors are equally weighted. Instead, in this study, NARX models were trained by modifying the performance function reported in Eq. (2) to the form expressed in Eq. (3), so that each term can be properly weighted:

$$F_c = mse = \frac{1}{n}\sum_{i=1}^{n}c_i^2\left(e_i\right)^2 = \frac{1}{n}\sum_{i=1}^{n}c_i^2\left(y_{mi} - y_{si}\right)^2 \qquad (3)$$

Equation (4) represents the EWF which must have the same dimensions as the output data and should assume values in the range [0; 1].

$$EWF = c_i = g(TR) \qquad i = 1,2,3,\ldots,n \qquad (4)$$

The EWF depends on data topology of which an example is provided in the next section. EWF can be selected so that the errors in some parts of each training sequence contribute more to the weighted performance function F_c than the errors in other parts of each training sequence.

Sensitivity analysis

The selection of the number of neurons depends on the characteristics of the system to be modeled, the number of input and output signals and the amount of training datasets within the selected range of variations of inputs and outputs.

As reported in Fig. 1, the number of neurons in the hidden layer should be identified by means of a sensitivity analysis by considering NARX models with a different number of neurons. Then, for every number of neurons, a sensitivity analysis on the initial weights should be carried out.

Different values of initial weights can lead to various solutions. To avoid local minimum problems, for every number of neurons, several networks can be trained starting from different random initial weights. Namely, it was found out that the initial random weights should be generated so that all sigmoid nodes are in their linear region. Otherwise, nodes can be initialized into flat regions of the sigmoid causing very small gradients. Therefore, an optimal set of initial weights can be identified.

Once the optimal number of neurons and the initial weights are identified, the NARX models with the best training performance are also identified and tested against additional time series.

The parameter which was used to compare the measured data (y_m) to NARX model predictions (y_s) is the *root mean square relative error* (*RMSE*) defined according to Eq. (5):

$$RMSE = \sqrt{\frac{1}{n}\sum_{i=1}^{n}\left(e_{R,i}\right)^2} = \sqrt{\frac{1}{n}\sum_{i=1}^{n}\left(\frac{y_{mi} - y_{si}}{y_{mi}}\right)^2} \qquad (5)$$

where *n* is the number of data in each dataset.

CASE STUDY

Gas turbine specifications

The gas turbine modeled in this paper is the General Electric PG 9351FA. It is a heavy-duty single-shaft gas turbine used for power generation. The main specifications are summarized in Table 1.

Table 1 – Gas turbine design specifications

GT type	GE 9351FA
Number of shafts	1
Rotational speed	3000 rpm
Pressure ratio	15.8
TIT	1327 °C
TOT	599 °C
Air flow rate	648 kg/s
Power	259.5 MW
Heat rate	9643 kJ/kWh
Efficiency	37.3 %

Set-up of the training methodology

Selection of the training datasets. As previously discussed, the first step of the training methodology requires an accurate selection of the training datasets.

In this study, the datasets used for the set-up and validation of the NARX models were taken experimentally during several start-up maneuvers and cover the whole operating range and conditions of the gas turbine during start-up. Moreover, they consider all the conditions relating to this type of transient operation (e.g. bleed valve opening, IGV control, etc.).

The datasets used were taken experimentally during several start-up maneuvers and cover the whole operational range of the GT during cold, warm and hot start-up.

The datasets during start-up can be categorized as follows:

- cold start-up: the gas turbine was shut down some days before start-up;
- warm start-up: the gas turbine was shut down some hours before start-up;
- hot start-up: the gas turbine was shut down just few hours or less before start-up.

The six measured time series datasets which were used for NARX model training are called $TR1_C$, $TR2_C$, $TR3_C$, $TR4_C$, $TR5_C$ and $TR6_C$ for cold start-up and $TR1_W$, $TR2_W$, $TR3_W$, $TR4_W$, $TR5_W$ and $TR6_W$ for warm start-up. Instead, for hot start-up, only two datasets ($TR1_H$ and $TR2_H$) were used for model training.

The datasets cover the whole operating range of the gas turbine during start-up and they were selected in such a manner that the resulting model can generalize well for GT simulation during start-up. In fact, the datasets ($TE1_C$, $TE2_C$, $TE3_C$, $TE4_C$, $TE5_C$ and $TE6_C$ for cold start-up, $TE1_W$, $TE2_W$, $TE3_W$, $TE4_W$, $TE5_W$ and $TE6_W$ for warm start-up and $TE1_H$ for hot start-up) used to test and validate the trained models are included in the operating range of the training datasets. More details concerning the operating range for the two input parameters of the training datasets are shown in Table 2 and Table 3. It should be noticed that data sampling frequency is 1 s.

Table 2 – Number of datasets in training and testing maneuvers

TR1	TR2	TR3	TR4	TR5	TR6	TE1	TE2	TE3	TE4	TE5	TE6
				Cold start-up							
478	428	461	484	478	478	483	482	482	480	461	479
				Warm start-up							
453	480	477	479	462	478	428	478	429	429	482	448
				Hot start-up							
396	403	-	-	-	-	403	-	-	-	-	-

Table 3 – Operational range of the inputs

Start-up category	T_{01} [K]	M_f [kg/s]
Cold start-up	[282.6; 307.6]	[0.26; 4.92]
Warm start-up	[280.4; 298.2]	[0.36; 4.93]
Hot start-up	[293.2; 302.6]	[0.36; 4.69]

It can be seen from Fig. 2 that the trends of all maneuvers are similar, but the rate of change of the rotational speed to reach the full speed/no-load condition is different. Therefore, as discussed while describing the training methodology, in order to set up a robust NARX model, the rate of change of the fuel mass flow rate of the maneuvers used for training must include the most rapid variation ($TR1_C$, $TR1_W$ and $TR1_H$) and the slowest variation ($TR6_C$, $TR6_W$ and $TR2_H$), as shown in Figure 2.

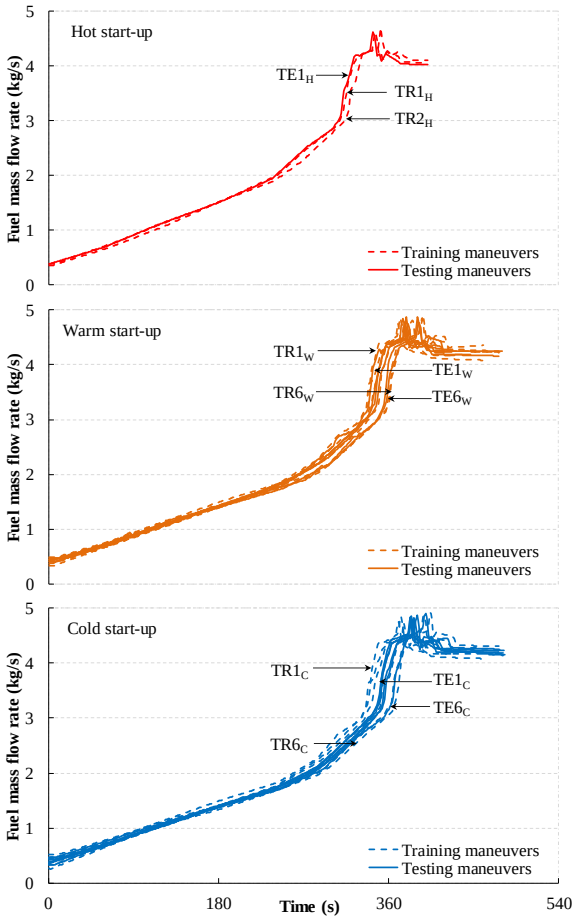

Figure 2 – Trend over time of the fuel mass flow rate during hot (top), warm (middle) and cold (bottom) start-up

In this study, the NARX models were created by using the Neural Network Toolbox of MATLAB©.

According to the methodology sketched in Figure 1, to train the NARX models, six measured time series datasets ($TR1_C$ through $TR6_C$) were selected for cold start-up, six additional measured time series datasets ($TR1_W$ through $TR6_W$) for warm start-up and two additional datasets ($TR1_H$ and $TR2_H$) for hot start-up.

Definition of the error weight function. Different EWFs were analyzed in a previous work by the same authors [20]. In this paper, as shown in Figure 3 and according to Eq. (6), the EWF follows the same trend of the training datasets (for each output variable), normalized in the range [0.1; 1]. Namely, the terms in Eq. (3) are weighted so that the squared error associated to the minimum value of each output variable (i.e. T_{04}, T_{02}, P_{rC} and N) has a weight of 0.1 and the squared error associated to the maximum value has a weight of 1.0. Different tests were made on different normalization intervals, and the NI [0.1; 1] proved to be the best. Also, the factor ($NI_{max} - NI_{min}$) in Eq. (6) is required to scale the weights in the normalization interval.

$$EWF = \begin{cases} c_i = (NI_{\max} - NI_{\min}) * \left[\dfrac{y_{mi} - y_{m\min}}{y_{m\max} - y_{m\min}} \right] + NI_{\min} \\ NI_{\min} = 0.1 \quad ; \quad NI_{\max} = 1 \quad ; \quad i = 1,2,3,...,n \end{cases} \qquad (6)$$

In order to force the NN to reproduce the most relevant parts of the maneuvers, the EWF was selected so that the errors in the last part of each training sequence (i.e. when steady-state conditions are almost reached) contribute more to the weighted performance function than the errors in the initial part of each training sequence (i.e. when purely transient conditions occur).

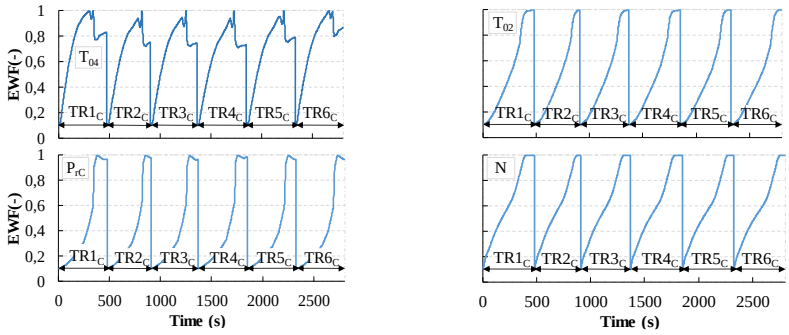

Figure 3 – EWF for T_{04}, T_{02}, P_{rC} and N for cold start-up

Sensitivity analysis. As shown in Fig. 1, once the training datasets are selected and the EWF is defined, a sensitivity analysis on the number of neurons and initial weights is required. The optimal number of neurons in the hidden layer is assumed to be 12 in this paper, according to the sensitivity analysis carried out in a previous work [20], where the performance of NARX models with 6, 12 and 18 neurons was extensively analyzed.

Once the number of neurons is frozen (i.e. 12 neurons), in order to carry out the sensitivity analysis on the initial weights, the training process was repeated several times by initializing the neural network with different initial weights. Each time the initial random weights are generated by using a standard uniform distribution between -0.5 and 0.5 and for every output variable (i.e. T_{04}, T_{02}, P_{rC} and N) five guesses of initial weights were set for the training of the neural network (Figures 6 through 8). The process was repeated for cold, warm and hot start-up. It should be noticed that the RMSE calculated over all the training datasets was considered the only target parameter, since the training time was similar in all cases (less than one minute). Furthermore, to account for the initial delay of the NARX model to work correctly, the values corresponding to the first ten seconds of each dataset were not used for RMSE calculation.

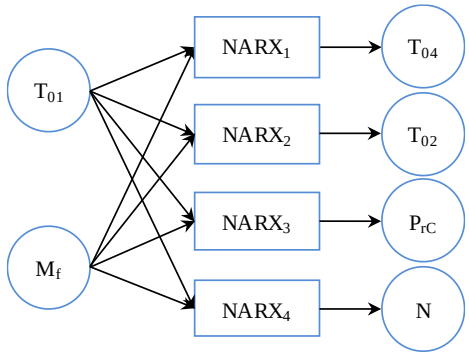

Figure 4 – Block diagram of the complete NARX model

As shown in Fig. 4, each NARX model has a multi-input single-output structure, which consists of two inputs and one output. The input variables $x(t)$ are the compressor inlet temperature T_{01} and the fuel mass flow rate M_f. The output variables $y(t)$ are the turbine outlet temperature T_{04}, the compressor outlet temperature T_{02}, the compressor pressure ratio P_{rC} and the rotational speed N.

The training of all NARX models was made by considering an open loop structure, as shown in Fig. 5.

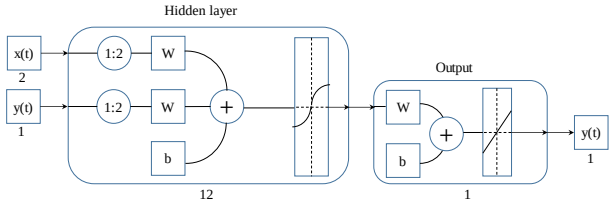

Figure 5 – Open-loop structure of a NARX model

The NARX models were trained by using the *Bayesian regularization* training algorithm (*trainbr*), one hidden layer and tapped delay lines with two delays (1:2) both for inputs $x(t)$ and output $y(t)$. This means that the previous time steps are $(t\text{-}1)$ and $(t\text{-}2)$, according

to the analysis performed in [18].

The two initial values (at time points t = 1 s and t = 2 s) of the two inputs and four outputs were calculated as in Eq. (7):

$$\phi_{average}(t) = \sum_{j=1}^{k} \frac{\phi_{TRj}(t)}{k}; \qquad k = k_{TR} \qquad t = 1,\ 2 \qquad (7)$$

As it can be seen, the initial values at time points 1 s and 2 s were selected to be the average of the corresponding values in the six (k=6) transients used for training ($TR1_C$ through $TR6_C$) for cold start-up and ($TR1_W$ through $TR6_W$) for warm start-up. Instead two (k=2) transients are used for training ($TR1_H$ and $TR2_H$) for hot start-up. This was a pragmatic approach, since these values are always known to NARX users. These values are reported in Table 4.

Table 4 – Inputs and outputs averaged values

Time (s)	*Input variables x*		*Output variables y*			
	$T_{01,av}$ (K)	$M_{f,av}$ (kg/s)	$T_{04,av}$ (K)	$T_{02,av}$ (K)	$P_{rC,av}$ (-)	N_{av} (rpm)
			Cold start-up			
1	295.4	0.39	505.3	303.2	1.07	421.5
2	295.4	0.40	506.5	303.2	1.07	424.8
			Warm start-up			
1	288.4	0.43	504.9	297.5	1.11	421.8
2	288.4	0.43	506.0	297.5	1.11	424.3
			Hot start-up			
1	295.6	0.37	565.1	310.9	1.06	421
2	295.6	0.37	566.2	310.9	1.06	423

Figures 6 through 8 show the training performance of the NARX models for cold, warm and hot start-up, respectively. It can be seen that different initial weights can lead to different RMSE values, mainly for the output P_{rC}, which has the higher RMSE. Otherwise, the influence of initial weights on the other outputs (i.e. T_{04}, T_{02} and N) is lower.

The Table 5 reports the values of the *overall* (Ov) RMSE values calculated on all the training maneuvers and also the minimum and maximum (Min and Max) RMSE value. It should be mentioned that the RMSE values reported in Table 5 were calculated for the NARX models with the best training performance (i.e. with minimum RMSE).

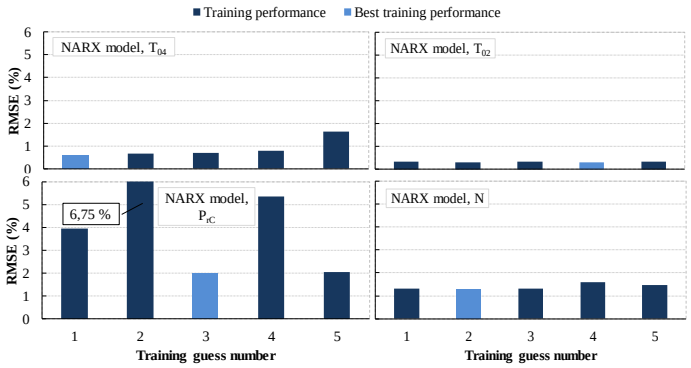

Figure 6 – RMSE of trained NARX models for cold start-up

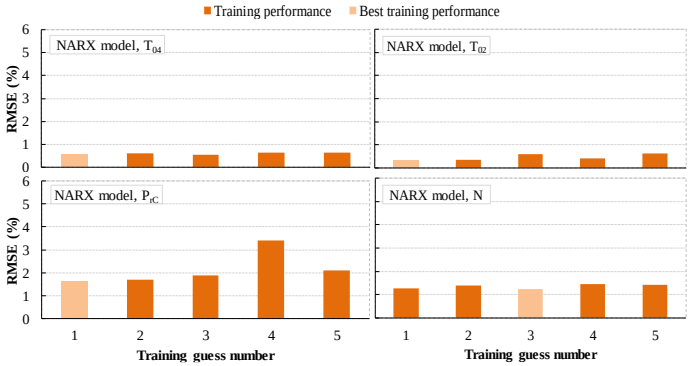

Figure 7 – RMSE of trained NARX models for warm start-up

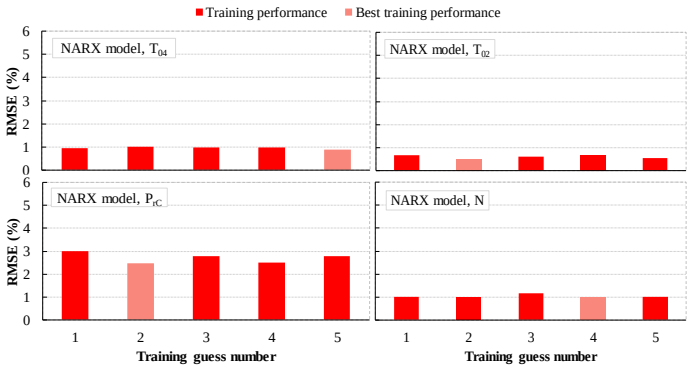

Figure 8 – RMSE of trained NARX models for hot start-up

It can be observed that the overall RMSE values depend on the considered variable. In fact, the RMSE values of T_{04} and T_{02} are smaller than P_{rC} and N. In particular, higher RMSE values were calculated for P_{rC}. However, training is clearly satisfactory for all outputs and all the types of start-up maneuvers. In fact, all RMSE values are lower than 2.5%. The NARX models with the RMSE values obtained were considered accurate and the training phase were considered satisfactory. Finally, it is worth highlighting that, during the training phase, the training datasets were provided to the NARX models in sequence, since all data have to be supplied contemporarily for training. Instead, the simulations performed in the next Section were conducted by simulating the training maneuvers one by one.

Table 5 – RMSE of the best trained NARX models

Start-up	RMSE [%]							
	T_{04}		T_{02}		P_{rC}		N	
	Ov	MinMax	Ov	MinMax	Ov	MinMax	Ov	MinMax
Cold	0.6	[0.4-0.8]	0.3	[0.2-0.8]	2.0	[1.3-2.6]	1.3	[0.8-1.8]
Warm	0.5	[0.3-0.7]	0.3	[0.2-0.6]	1.6	[1.3-2.1]	1.2	[0.6-1.7]
Hot	0.9	[0.5-1.2]	0.5	[0.4-0.6]	2.5	[1.4-3.2]	1.0	[0.8-1.2]

NARX model validation

The best trained NARX models for cold, warm and hot start-up were tested against additional experimental datasets. Namely, $TE1_C$ through $TE6_C$ and $TE1_W$ through $TE6_W$ for cold and warm start-up respectively and $TE1_H$ for hot start-up.

For simulation and testing, a closed loop structure (Figure 9) was adopted. This means that the NARX model is fed with the values estimated by itself at antecedent time steps.

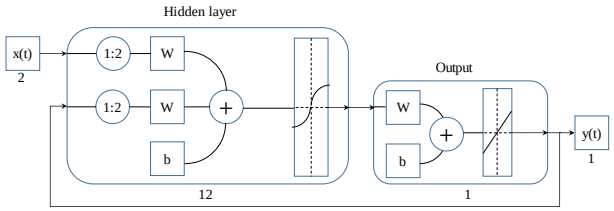

Figure 9 – Closed-loop structure of a NARX model

The prediction was performed by starting from two averaged initial conditions (see Table 4). Also in this case, to account for the initial delay of the NARX model to work correctly, the values corresponding to the first ten seconds of each dataset are not used for RMSE calculation. The results in terms of RMSE are summarized in Table 6, which directly compares the RMSE values obtained during testing (TE) and the corresponding values obtained during training (TR).

Table 6 – RMSE calculated on training and testing datasets

	RMSE [%]							
Start-up Category	T_{04}		T_{02}		P_{rC}		N	
	TR	TE	TR	TE	TR	TE	TR	TE
Cold	0.6	1.2	0.3	0.6	2.0	2.0	1.3	1.6
Warm	0.5	1.2	0.3	0.7	1.6	2.1	1.2	2.0
Hot	0.9	1.0	0.5	0.5	2.5	3.8	1.0	2.6

It can be observed that the RMSE values for T_{04}, T_{02}, P_{rC} and N are slightly higher than the corresponding values obtained during training (see Table 6). This means that the trained NARX models have good generalization capability, except for P_{rC} and N during hot start-up. This can be explained by the fact that the NARX models for hot start-up were trained by using only two training datasets. Despite this, the RMSE values are still acceptable. The trend of the testing maneuvers over time and the corresponding relative error are reported in Appendix A, together with a discussion about NARX model capabilities.

CONCLUSIONS

This paper presented a methodology for the development of NARX neural network models, in order to simulate the dynamic behavior of a heavy-duty gas turbine during start-up. The NARX models were trained by using 14 measured time series (6 for cold start-up; 6 for warm start-up; 2 for hot start-up). For validation purposes, the trained NARX models were tested against 13 measured time series (6 for cold start-up; 6 for warm start-up; 1 for hot start-up), all of them different from the ones used for training.

During the training phase, the neural network performance function was modified, so that every term is properly weighted by means of an error weight function. A sensitivity analysis on the initial weights was also performed.

In all simulations (during both training and testing), no significant deviations occurred between simulated and measured data. The RMSE values during the training phase were satisfactory, i.e. below 2% for three outputs and equal to 2.5% only for the compressor pressure ratio during hot start-up. Anyway, this latter value can still be considered satisfactory. During the testing phase, the RMSE values proved acceptable, i.e. in the range 0.6% - 2.0% for cold start-up, 0.7% - 2.1% for warm start-up and 0.5% - 3.8% for hot start-up. The reason for the higher value in the latter case is that only two training datasets were used for hot start-up training.

In summary, the NARX model developed in this paper proved very robust to reproduce the unsteady behavior and capture system dynamics. Moreover, this paper demonstrated the effectiveness of the methodology set-up in this paper to achieve the final optimal NARX models. The methodology presented in this paper is general, while results are specific to the considered case study. The extension of the results presented in this paper to other systems can be performed by exploiting the general guidelines for tuning NARX models reported in this paper, but training on the system under consideration should be made by considering its specific characteristics.

REFERENCES

[1] Jelali M, Kroll A. Hydraulic servo-systems: modeling, identification, and control. Springer Publications; 2004.

[2] Nikpey H., Assadi M., Breuhaus P., 2013, “Development of an optimized artificial neural network model for combined heat and power micro gas turbines”, Applied Energy, 108, pp. 137-148.

[3] Sisworahardjo N., El-Sharkh M. Y., 2013, “Validation of Artificial Neural Network Based Model of Microturbine Power Plant” , IEEE, doi: 10.1109/IAS.2013.6682526.

[4] Jingzhou F., Ningbo Z., Yong S., Yongming F., Zhongwei W., 2016, “Compressor performance prediction using a novel feed-forward neural network based on Gaussian kernel function”, Advances in Mechanical Engineering, 8, pp. 1-14.
[5] Lazzaretto A, Toffolo A. Analytical and neural network models for gas turbine design and off-design simulation. International Journal of Applied Thermodynamics 2001; Vol. 4, No. 4, pp.173-182.
[6] Ogaji S O T, Singh R, Probert S D. Multiple-sensor fault-diagnosis for a 2-shaft stationary gas turbine. Applied Energy2002; Vol. 71, No. 4, pp.321-339.
[7] Arriagada J, Genrup M, Loberg A, Assadi M. Fault diagnosis system for an industrial gas turbine by means of neural networks. In: Proceedings of the International Gas Turbine Congress, Tokyo, Japan; 2003.
[8] Basso M, Giarre L, Groppi S, Zappa G. NARX models of an industrial power plant gas turbine. IEEE Transactions on Control Systems Technology 2004; Vol. 13, No. 4, pp.599-604.
[9] Bettocchi, R., Pinelli, M., Spina, P. R., Venturini, M., Burgio, M., 2004, “Set up of a Robust Neural Network for Gas Turbine Simulation”, ASME Paper GT2004-53421.
[10] Bettocchi, R., Pinelli, M., Spina, P. R., Venturini, M., 2007, “Artificial Intelligence for the Diagnostics of Gas Turbines. Part II: Neuro-Fuzzy Approach”, ASME J Eng Gas Turb Power, 129(3), pp. 720-729.
[11] Spina, P. R., Venturini, M., 2007, “Gas Turbine Modeling by Using Neural Networks Trained on Field Operating Data”, Proc. ECOS 2007, June 25 – 28, Padova, Italy, SGE Ed., Padova, Vol. I, pp. 213-222.
[12] Simani S, Patton R J. Fault diagnosis of an industrial gas turbine prototype using a system identification approach. Control Engineering Practice2008; Vol. 16, No. 7, pp.769-786.
[13] Yoru Y, Karakoc T H, Hepbasli A. Application of artificial neural network (ANN) method to exergetic analyses of gas turbines. International Symposium on Heat Transfer in Gas Turbine Systems2009; Antalya, Turkey.
[14] Fast M, Assadi M, De S. Condition based maintenance of gas turbines using simulation data and artificial neural network: A demonstration of feasibility. ASME Paper GT2008-50768.
[15] Fast M, Palme T, Karlsson A. Gas turbines sensor validation through classification with artificial neural networks. Brazil; ECOS 2009.
[16] Fast M, Palme T. Application of artificial neural network to the condition monitoring and diagnosis of a combined heat and power plant. Journal of Energy 2010; Vol. 35, No. 2, pp.1114-1120.
[17] Fast M. Artificial neural networks for gas turbine monitoring, Doctoral Thesis, Division of Thermal Power Engineering, Department of Energy Sciences, Faculty of Engineering, Lund University, Sweden; 2010.
[18] Asgari, H., Chen, X., Morini, M., Pinelli, M., Sainudiin, R., Spina, P. R., Venturini, M., 2016, “NARX models for simulation of the start-up operation of a single-shaft gas turbine”, Applied Thermal Engineering, 93, pp. 368-376.
[19] Asgari, H., Venturini, M., Chen, X., Sainudiin, R., 2014, “Modeling and Simulation of the Transient Behavior of an Industrial Power Plant Gas Turbine”, J. Eng. Gas Turbines Power 136(6), 061601 (10 pages), doi: 10.1115/1.4026215.
[20] Bahlawan, H., Morini, M., Pinelli, M., Spina, P. R., Venturini, M., 2016, “Set-up of a Robust Narx Model Simulator of Gas Turbine Start-up”, *Proc. ECOS 2016*, June 19th – 23rd, Potoroz, Slovenia, *Paper 257*.
[21] Dominiczak K., Rzadkowski R., Radulski W., Szczepanik R., On-line prediction of temperature and stress in steam turbine components using neural networks. ASME J Eng Gas Turb Power 138(5), 052606; doi: 10.1115/1.4031626.
[22] Vatani A., Khorasani K., Meskin N., Health monitoring and degradation prognostics in gas turbine engines using dynamic neural networks. ASME Paper GT2015-44101.
[23] Amozegar M., Khorasani K., 2016, “An ensemble of dynamic neural network identifiers for fault detection and isolation of gas turbine engines”, Neural Networks, 76, pp. 106-121.
[24] Chaibakhsh A., Amirkhani S., Piredeir P., 2015, “Temperature Sensor Fault Diagnosing in Heavy Duty Gas Turbines Using Laguerre Network-Based Hierarchical Fuzzy Systems”, IEEE, doi:10.1109/INISTA.2015.7276768.
[25] Lakshmi K., Sunny H., Ramesh Babu N., Neural network based estimation of gas turbine engine. Global Journal of Pure and Applied Mathematics 2015;11(6):4365-4374.
[26] Sina Tayarani-Bathaie S., Khorasani K., Fault detection and isolation of gas turbine engines using a bank of neural networks. Journal of Process Control 2015;36:22-41.
[27] Tsoutsanis E., Meskin N., Benammar M., Khorasani K., A dynamic prognosis scheme for flexible operation of gas turbines. Applied Energy 2016;164:686-701.
[28] Tavakolpour-Saleh A.R., Nasib S.A.R., Sepasyan A., Hashemi S.M., 2015, “Parametric and nonparametric system identification of an experimental turbojet enjine”, Aerospace Science and Technology, 43, pp. 21-29.
[29] Venturini, M., 2006, “Simulation of Compressor Transient Behavior Through Recurrent Neural Network Models”, ASME J Turbomach, 128(3), pp. 444-454.
[30] Venturini, M., 2007, “Optimization of a Real-Time Simulator Based on Recurrent Neural Networks for Compressor Transient Behavior Prediction”, ASME J Turbomach, 129(3), pp. 468-478.
[31] Venturini, M., 2005, “Development and Experimental Validation of a Compressor Dynamic Model”, ASME J Turbomach, 127(3), pp. 599-608. Erratum printed on ASME J. of Turbomachinery, 128(1).

[32] Morini, M., Pinelli, M., Venturini, M., 2007, "Development of a One-Dimensional Modular Dynamic Model for the Simulation of Surge in Compression Systems", ASME J Turbomach, 129(3), pp. 437-447.
[33] Morini, M., Pinelli, M., Venturini, M., 2009, "Analysis of Biogas Compression System Dynamics", Applied Energy, 86, pp. 2466-2475.
[34] Nowak G., Rustin A., 2016, "Using the artificial neural network to control the steam turbine heating process", Applied Thermal Engineering, 108, pp. 204-210.
[35] Morini, M., Cataldi, G., Pinelli, M., Venturini, M., 2007, "A Model for the Simulation of Large-Size Single-Shaft Gas Turbine Start-Up Based on Operating Data Fitting", ASME Paper GT2007-27373.
[36] Walsh, P P, Fletcher P. Gas turbine performance. Blackwell Science Ltd, UK; 1998.
[37] Hudson Beale M, T Hagan M, B Demuth H. Neural network tool boxTM user's guide, R2013a, The MathWorks, Inc., USA; 2013.

APPENDIX A. TREND OF TESTING MANEUVERS

The Figures A.1 through A.5 show the trend-over-time of the testing maneuvers during cold, warm and hot start-up, respectively. In all cases, the trends of the field data and NARX predictions are very similar. This means that the NARX models can follow the changes in GT parameters, even though they are subject to significant changes. Furthermore, it can be clearly seen that the quasi steady-state operation in the last phase of each maneuver can also be reproduced accurately.

Therefore, it can be concluded that the NARX models reproduce the testing datasets during cold, warm and hot start-up accurately. In other words, they can generalize well.

Finally, it should be noticed that, on average, the NARX models developed in this paper can reproduce the GT dynamic behavior more accurately (i.e. with lower RMSE values) than the NARX models presented by the same authors in previous work [20]. More in detail, with reference to cold start-up, by comparing the RMSE values calculated for testing maneuvers, it can be observed that RMSE values for T_{04}, T_{02}, P_{rC} and N are decreased from 3.0%, 0.8%, 3.2% and 2.7% to 1.2%, 0.6%, 2.0% and 1.6% respectively, thanks to the optimization of the training phase performed in this paper.

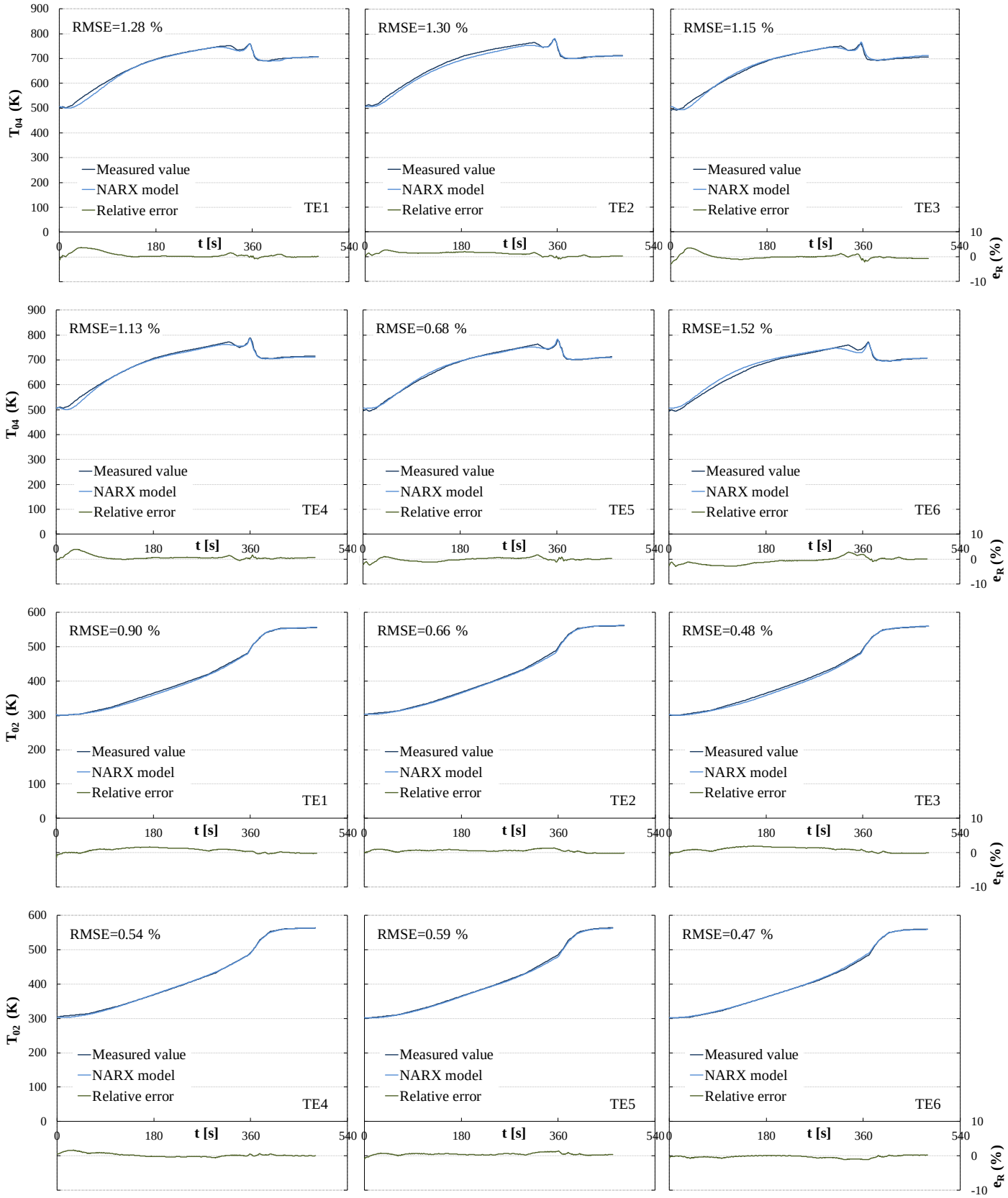

Figure A.1 – Trend of T_{04} and T_{02} for the testing maneuvers during cold start-up

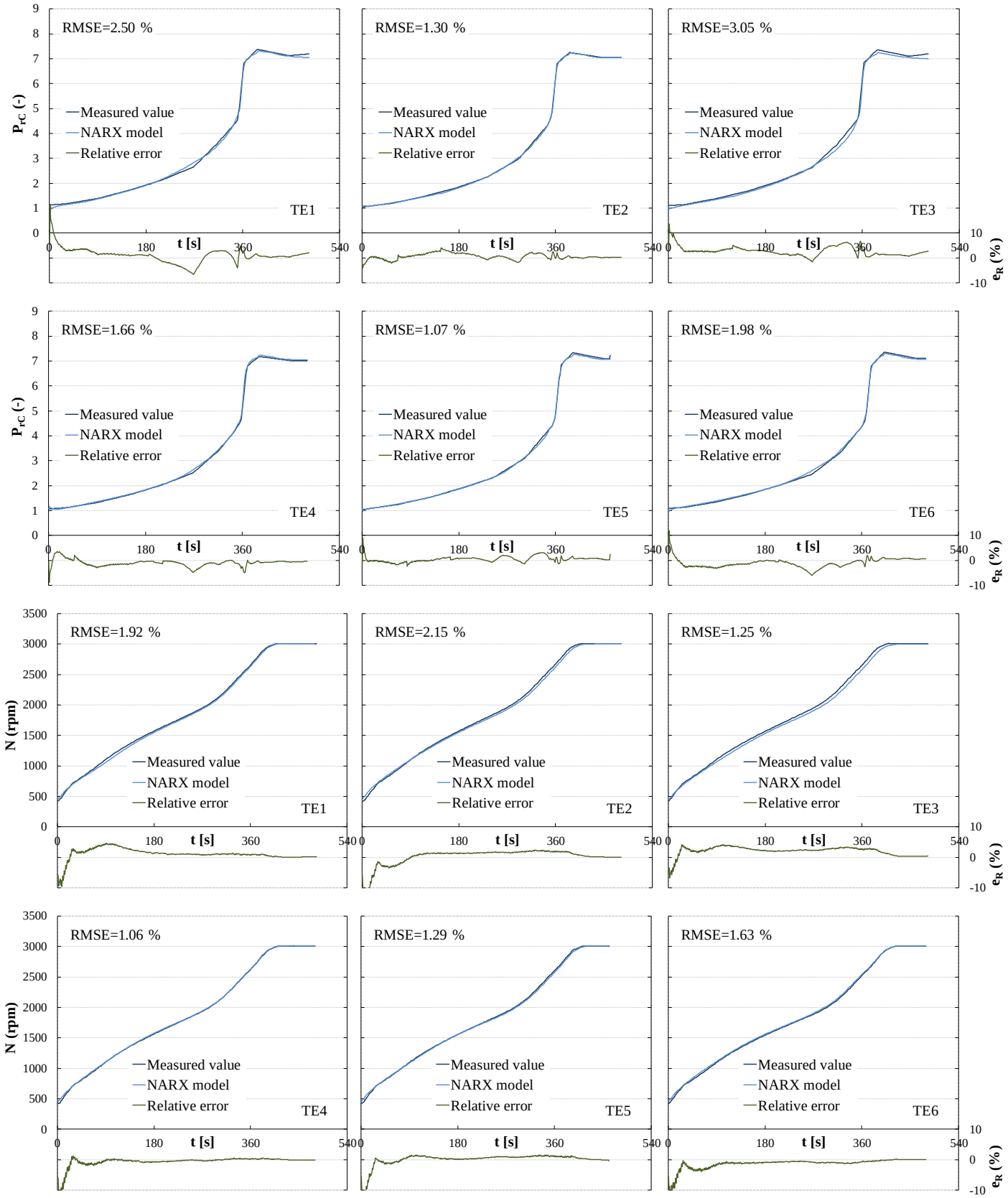

Figure A.2 – Trend of P_{rC} and N for the testing maneuvers during cold start-up

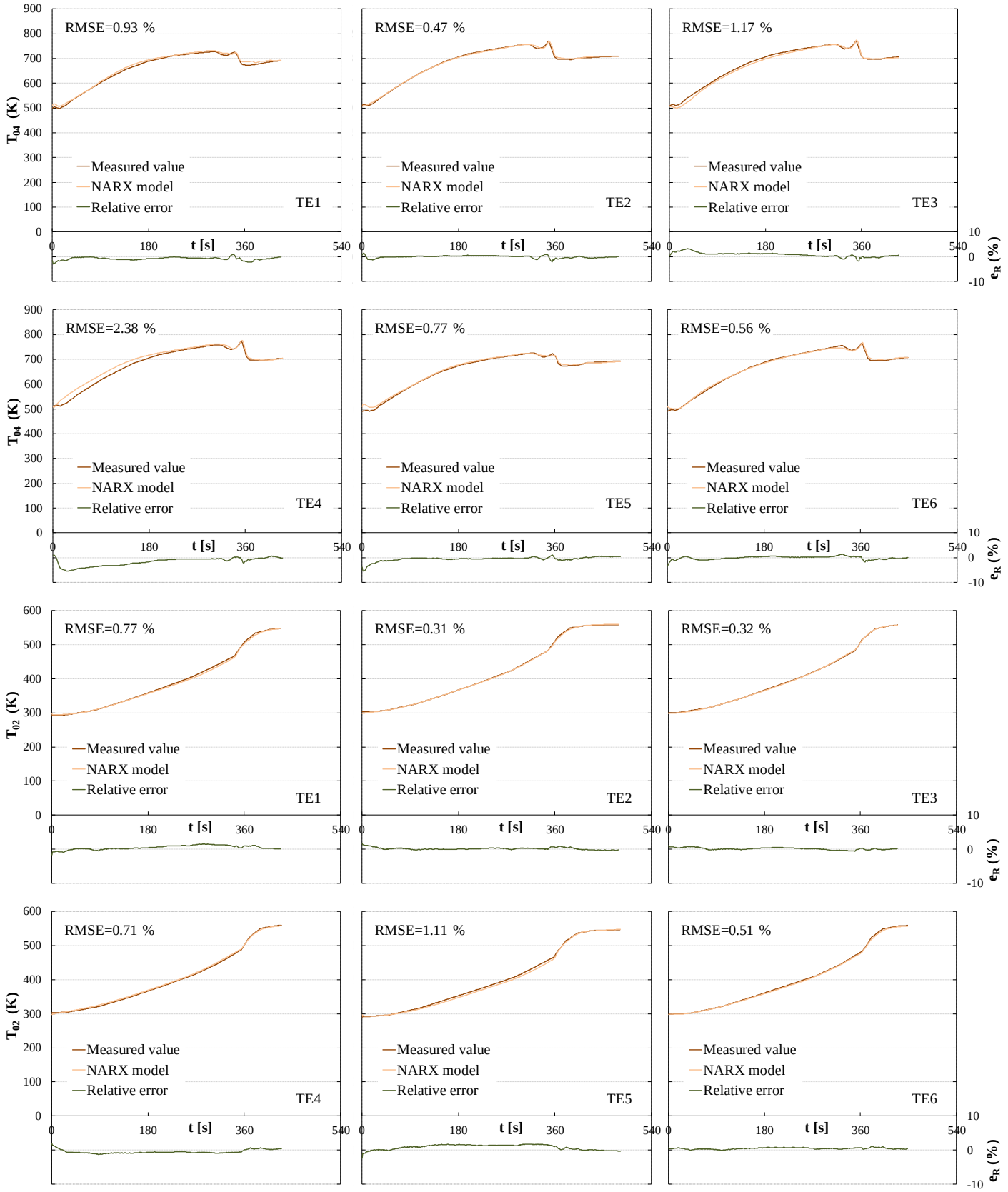

Figure A.3 – Trend of T_{04} and T_{02} for the testing maneuvers during warm start-up

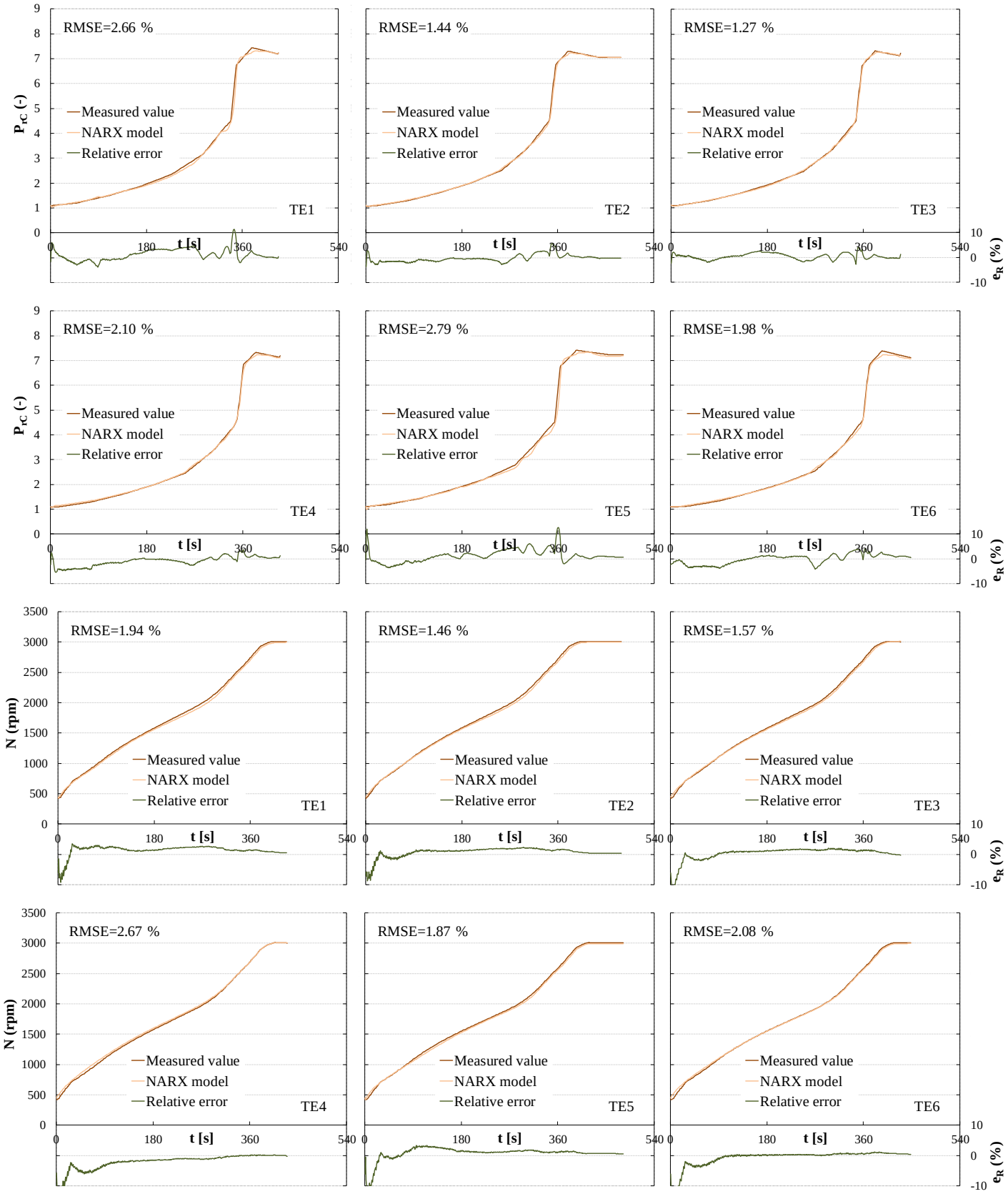

Figure A.4 – Trend of P_{rC} and N for the testing maneuvers during warm start-up

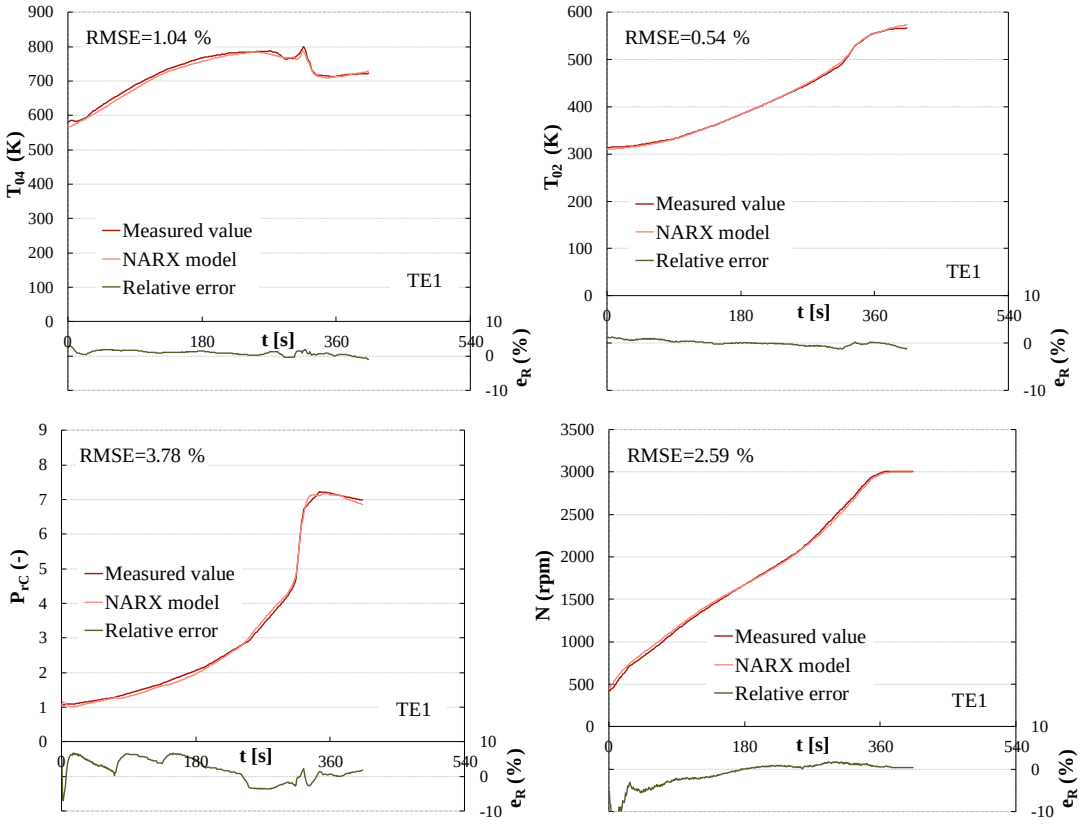

Figure A.5 – Trend of T_{04}, T_{02}, P_{rC} and N for the testing maneuver TE1 during hot start-up

List of figure captions

List of table captions